

Role of dynamical non-double-occupancy excitations on the quasiparticle damping of the $t - J$ model in the large- N limit

A. Foussats, A. Greco, and M. Bejas

† *Facultad de Ciencias Exactas, Ingeniería y Agrimensura and Instituto de Física Rosario (UNR-CONICET). Av. Pellegrini 250-2000 Rosario-Argentina.*

(Dated: November 29, 2018)

One-electron self-energy in the t - J model was computed using a recently developed large- N method based on the path integral representation for Hubbard operators. One of the main features of the self-energy is its strong asymmetry with respect to the Fermi level, showing the spectra mostly concentrated at high negative energy. This asymmetry is responsible for the existence of incoherent structures at high negative energy in the spectral functions. It is shown that dynamical non-double-occupancy excitations are relevant for the behavior of the self-energy. It is difficult to understand the asymmetry shown by the self-energy from weak coupling treatments. We compare our results with others in recent literature. Finally, the possible relevance of our results for the recent high energy features observed in photoemission experiments is discussed.

PACS numbers: 71.10.Fd, 71.27.+a, 74.72.-h

It is commonly accepted that high- T_c cuprates are strongly correlated systems. In these materials angle resolved photoemission spectroscopy (ARPES) experiments show interesting and still unexplained features: a) the low energy kink¹ at energy $\sim 40 - 70 meV$ and; b) the high energy anomalies^{2,3,4,5,6} at $\sim 0.5 - 1 eV$, known as waterfall. For a theoretical description of these experiments it is necessary to calculate self-energy corrections on electronic correlated models as $t - J$ or Hubbard. In spite of the progress by means of numerical⁷ and analytical⁸ methods, the problem remains of huge interest. Recently we have proposed a large- N approach⁹ for the $t - J$ model which is based on the path integral representation for Hubbard operators (called PIH in what follows). In the PIH method the spin index σ is extended to a new index p running from 1 to N and the perturbation is performed in powers of the small parameter $1/N$. It was shown that in leading order of $1/N$ ($\mathcal{O}(1)$), which is equivalent to mean field level, PIH results agree with the slave boson⁸ calculation. The large- N expansion provides a controllable way for selecting and truncating Feynman diagrams. However, the results are more representative for the physical case $N = 2$ when terms in powers of $1/N$ can be collected. In this context, PIH can be implemented beyond mean field allowing the calculation of self-energy corrections and spectral functions.^{10,11} The obtained spectral functions were compared with exact diagonalization results finding good agreement.^{10,11}

In this paper we discuss the role of dynamical fluctuations of the non-double-occupancy constraint on the self-energy results. In addition, differences between present self-energy and that obtained from calculations based on weak coupling approaches like, for instance, random phase approximation¹² (RPA) are discussed. We compare also our results with those obtained by other calculations, and discuss the possible relevance of present results for the recent high energy features observed in ARPES experiments in cuprates.

In Refs.[9,10] it was discussed that PIH approach weak-

ens collective spin fluctuations over charge fluctuations. Although for finite doping away from half filling the relevance of magnetism is a matter of debate, for preventing possible objections about the influence of magnetic contributions, we calculate for the high doping value $\delta = 0.3$. This high doping corresponds to highly overdoped regime of cuprates where magnetic fluctuations are found to be very weak.¹³ In addition, and for simplicity, we present results for $J = 0$. For high doping, PIH does not show strong dependence with J , being representative the results for $J = 0$ (see Ref.[14] for discussion). On the other hand, no strong J dependence is expected for high doping values.

Collecting all $\mathcal{O}(1/N)$ contributions, the full self-energy $\Sigma(\mathbf{k}, \omega)$ (real and imaginary parts) in the square lattice is described in Refs.[10,11]. Herein, for convenience, we reproduce only the corresponding results for scattering rate:

$$\begin{aligned} \text{Im} \Sigma_T(\mathbf{k}, \omega) &= \text{Im} \Sigma_{RR}(\mathbf{k}, \omega) + 2 \text{Im} \Sigma_{R\lambda}(\mathbf{k}, \omega) \\ &+ \text{Im} \Sigma_{\lambda\lambda}(\mathbf{k}, \omega) \end{aligned} \quad (1)$$

where

$$\begin{aligned} \text{Im} \Sigma_{RR}(\mathbf{k}, \omega) &= \frac{-1}{N_s} \sum_{\mathbf{q}} \Omega^2 \text{Im}[D_{RR}(\mathbf{q}, \omega - \varepsilon_{k-q})] \\ &\times [n_F(-\varepsilon_{k-q}) + n_B(\omega - \varepsilon_{k-q})], \\ \text{Im} \Sigma_{R\lambda}(\mathbf{k}, \omega) &= \frac{-1}{N_s} \sum_{\mathbf{q}} \Omega \text{Im}[D_{\lambda R}(\mathbf{q}, \omega - \varepsilon_{k-q})] \\ &\times [n_F(-\varepsilon_{k-q}) + n_B(\omega - \varepsilon_{k-q})], \\ \text{Im} \Sigma_{\lambda\lambda}(\mathbf{k}, \omega) &= \frac{-1}{N_s} \sum_{\mathbf{q}} \text{Im}[D_{\lambda\lambda}(\mathbf{q}, \omega - \varepsilon_{k-q})] \\ &\times [n_F(-\varepsilon_{k-q}) + n_B(\omega - \varepsilon_{k-q})]. \end{aligned} \quad (2)$$

In eq.(2), $\Omega = (\varepsilon_{k-q} + \omega + 2\mu)/2$ and $\varepsilon_k = -t\delta(\cos k_x + \cos k_y) - \mu$ is the mean field electronic band. N_s is the

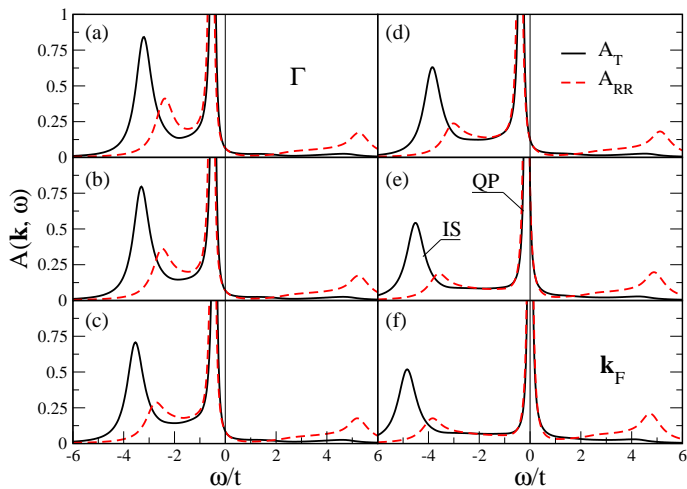


FIG. 1: (Color online) Spectral functions A_T (solid lines) and A_{RR} (dashed lines) from Γ (panel (a)) to \mathbf{k}_F (panel (f)) in the nodal direction for $\delta = 0.3$. Energies are in units of t . The vertical line at $\omega = 0$ marks the Fermi level.

number of sites, n_F (n_B) is the Fermi (Bose) factor and μ the chemical potential. $D_{RR}(\mathbf{q}, \omega)$ is the charge-charge correlation function which contains collective charge excitations. $D_{\lambda\lambda}$ and $D_{R\lambda}$ correspond to the pure non-double-occupancy sector and the mixing between non-double-occupancy and charge sectors respectively.

Starting from Σ_T and Σ_{RR} the spectral functions $A_T(\mathbf{k}, \omega)$ and $A_{RR}(\mathbf{k}, \omega)$ are respectively calculated. In the calculation of the spectral functions, the real part of Σ was numerically computed by using the Kramers-Kronig relation from eq.(1). Spectral functions $A_T(\mathbf{k}, \omega)$ (solid lines) are presented in Fig. 1 from Γ ($\mathbf{k} = (0, 0)$) (panel (a)) to the Fermi vector \mathbf{k}_F (panel (f)) in the $\Gamma - (\pi, \pi)$ direction (nodal direction) of the Brillouin zone (BZ). The sharp peak near $\omega = 0$ is the quasiparticle (QP) peak and defines the QP Zhang-Rice¹⁵ (ZR) band of the $t - J$ model whose bandwidth is reduced from that of the mean field band ε_k due to the self-energy renormalizations. In addition $A_T(\mathbf{k}, \omega)$ shows incoherent spectrum (IS) which is mainly localized at high negative energy ($\omega \sim -4t$). Almost no IS is observed for $\omega > 0$. Similarly to Lanczos diagonalization results,^{10,16,17} while the QP disperses through the Fermi surface, the IS moves in opposite direction. Present results are for temperature $T = 0K$, and a finite value for T does not change the main conclusion. As discussed below, self-energy contributions (Fig.3), responsible for the IS, lie on an energy scale of the order of several t . Therefore, no significant changes occur for realistic values of temperature.

Fig.2a shows, in the main directions of the BZ, the energy dispersion of the QP peak (solid circles) and the IS (open circles) shown by A_T . In panel (b) we reproduce the $t - J$ model results from Fig.1c of Ref.[18] obtained, also for doping $\delta = 0.3$, using Gutzwiller projection variational Monte Carlo (VMC). Although both

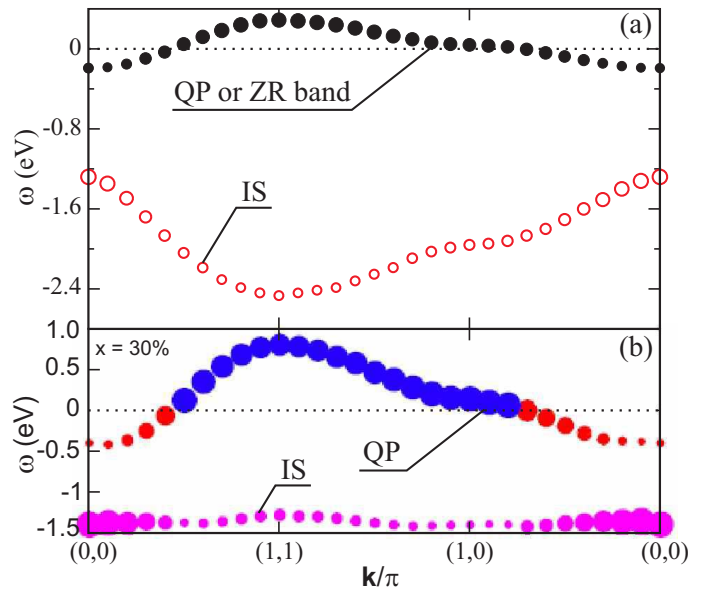


FIG. 2: (Color online) (a) Energy dispersion of the QP peak (solid circles) and the IS (open circles) shown by A_T for $\delta = 0.3$. (b) Results reproduced after Ref.[18] for a qualitative comparison with panel (a). Dotted line in both panels marks the Fermi level.

methods (PIH and VMC) are different, results are similar. Both panels show a QP (or ZR) band and IS at high negative energy. None of the obtained results show significant IS at positive energy. Although the IS is more dispersing in PIH than in VMC, its energy position is of the same order of magnitude in both methods. The QP band is somewhat flatter in PIH, if $t = 0.4eV$.¹⁸ For instance, the QP at Γ is at $\omega \sim -0.4eV$ for VMC and at $\omega \sim -0.2eV$ for PIH. (In Ref.[10] it was discussed that the QP bandwidth predicted by PIH is reduced from that obtained by Lanczos). The size of the circles scales linearly with the spectral weight (SW). The SW on the BZ is more homogeneous in panel (a) than in panel (b). PIH predicts, at \mathbf{k}_F , a QP weight $Z \sim 0.5$ indicating that, even for $\delta = 0.30$, $\sim 50\%$ of the SW is concentrated in the IS.

The scattering rate $-Im\Sigma_T(\mathbf{k}, \omega)$ at $\mathbf{k} = \mathbf{k}_F$ in the $\Gamma - (\pi, \pi)$ direction is presented in Fig. 3. $Im\Sigma_T$ (solid line) is very asymmetric with respect to $\omega = 0$ showing most of the SW at $\omega < 0$. This asymmetric behavior is the cause of the shape of A_T in Fig.1. This strong asymmetric distribution should be interpreted as a consequence of the difference between addition and removal of a single electron in a correlated system. Recently,¹⁹ using Lanczos diagonalization in the $t - J$ model, a similar asymmetric behavior was also discussed. It is important to notice that our scattering rate does not show any low energy scale, thus it can not explain the low energy kink. If the low energy kink is due to magnetic excitations,²⁰ or other electronic effects, they are obviously not include in our approach. However it is possible that the kink is

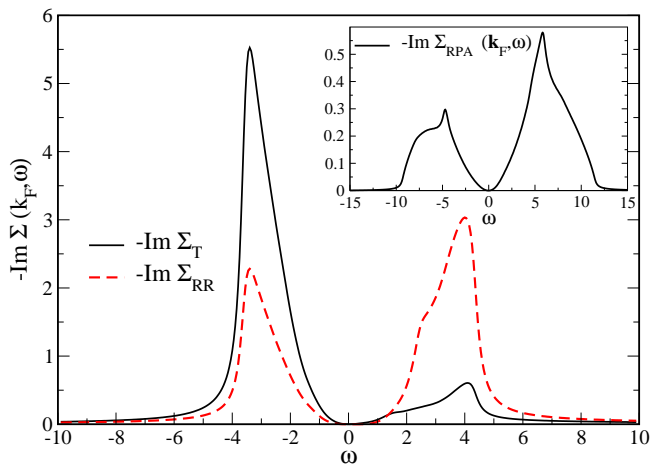


FIG. 3: (Color online) Scattering rate for Σ_T (solid line) and Σ_{RR} (dashed line) versus ω for $\delta = 0.3$ at $\mathbf{k} = \mathbf{k}_F$. Inset, scattering rate predicted by RPA on the Hubbard model for $\delta = 0.3$ at \mathbf{k}_F (see text).

due to phonons.²¹

For understanding which are the leading contributions responsible for the asymmetric behavior of Σ_T , we have calculated $-Im\Sigma_{RR}$. In contrast to $Im\Sigma_T$, $Im\Sigma_{RR}$ (dashed line in Fig.3) is very symmetric with respect to $\omega = 0$ and A_{RR} (dashed lines in Fig.1) shows the IS distributed almost equally at positive and negative ω . Evidently, $\Sigma_{R\lambda}$ and $\Sigma_{\lambda\lambda}$ (eq.(1) and eq.(2)) contribute significantly, showing the relevance of non-double-occupancy excitations on the redistribution of the SW for leading to the final form shown by A_T . In spite of the doping studied here corresponds to the highly overdoped regime of cuprates and it could be expected that a weak coupling approach, like RPA, be reliable, this is an open and controversial issue.²² For instance, and important for present discussion, ARPES experiments show, for highly overdoped samples, high energy anomalies with similar characteristics to those in underdoped samples.^{2,3,4,5,6} It is worth to mention that Σ_{RR} (first line in eq.(2)) has a somewhat similar meaning to the self-energy when only charge fluctuations are considered in RPA for the Hubbard model. This later can be written as²³

$$Im\Sigma_{RPA}(\mathbf{k}, \omega) = -\frac{1}{N_s} \sum_{\mathbf{q}} (U/2)^2 Im[\chi_c(\mathbf{q}, \omega - \xi_{k-q})] \times [n_B(\omega - \xi_{k-q}) + n_F(-\xi_{k-q})] \quad (3)$$

where χ_c is the RPA charge susceptibility,¹² U is the on-site Coulomb repulsion, and $\xi_k = -2t(\cos k_x + \cos k_y) - \mu$ is the bare tight-binding band on the square lattice. Since in both, $Im\Sigma_{RR}$ and $Im\Sigma_{RPA}$, charge excitations are involved in the electron renormalizations, it is instructive to compare results from both sides. Inset in Fig.3 shows $-Im\Sigma_{RPA}$ at the nodal \mathbf{k}_F for $U = 4$ and $\delta = 0.3$.

Interestingly, $Im\Sigma_{RPA}$ has a similar shape to that for $Im\Sigma_{RR}$, i.e., $-Im\Sigma_{RPA}$ is very symmetric with respect to $\omega = 0$, leading also (not shown) to IS homogeneously distributed at both sides of the Fermi level as for the case of A_{RR} (Fig.1). We have found this behavior for Σ_{RPA} very stable against different conditions for U and hole doping away from half-filling. Σ_{RR} and Σ_{RPA} show similarities because they can be simply interpreted in terms of fermions interacting with charge fluctuations. In our opinion this self-energy behavior, symmetrically distributed around $\omega = 0$, can be expected in weak coupling. However, results are different when the full self-energy (Σ_T) is considered. Σ_T is obtained in strong coupling and contains fluctuations above mean field level which are very difficult to be obtained perturbatively from usual fermions. The strong coupling calculation suggests that electrons interact with charge fluctuations and with excitations which represent non-double-occupancy effects. These excitations, expressed in our approach by $D_{R\lambda}$ and $D_{\lambda\lambda}$, are responsible of the concentration of the incoherent spectral weight at negative energy. In addition, they are dynamical (\mathbf{q} and ω dependent) and, they can not be simply considered as a static enforcement of non-double-occupancy constraint as in mean field approximation. At this point we wish to emphasize about the important role of the non-double-occupancy constraint even for the high doping studied here. In addition to the results in Ref.[18] for $\delta = 0.30$, Lanczos results¹⁷ for $\delta = 0.25$ show also large IS at negative ω . Since this behavior can be understood if the scattering rate is asymmetric with respect to $\omega = 0$, we think that these results indicate that the overdoped $t - J$ model shows strong coupling features. With increasing doping, our results will be closer to those obtained using RPA. For $\delta \gtrsim 0.7$, Σ_T becomes almost symmetric and, in this case, Σ_{RR} approaches Σ_T showing that $\Sigma_{R\lambda}$ and $\Sigma_{\lambda\lambda}$ have little influence.

Next, we discuss the possible relevance of present results for the high energy anomalies observed in ARPES experiments in cuprates. Momentum distribution curves (MDC) analysis of the experiment suggests the occurrence of one band which is strongly renormalized near the Fermi surface. Away from the Fermi surface this band develops an abrupt change reappearing at high energy ($\sim -1eV$), given the impression of a waterfall. This result supports a description in terms of renormalizations of the LDA^{3,5} or an uncorrelated band.²⁴ In contrast, energy distribution curves (EDC) analysis shows the simultaneous presence of both, low energy and high energy excitations.⁶ These results suggest the occurrence of a low energy band, associated with the ZR band of the $t - J$ model, and IS at high binding energy.^{18,19,25} Therefore, our results are in closer agreement with the interpretation obtained from the EDC analysis. At this point it is important to remark that it was recently discussed²⁶ that the waterfall dispersion is not an intrinsic feature but results from the suppression of the photoemission intensity near Γ due to matrix elements effects (see also Ref.[6] for discussion about the momentum and energy distribution

curves dichotomy). Concluding, we propose that the high energy features can be described in the framework of the $t - J$ model which shows the existence of a low energy ZR band and IS at high negative energy. Additionally, we have shown that dynamical non-double-occupancy excitations are relevant for transferring most of the SW to high negative energy, leading to a well pronounced IS at $\omega < 0$ as the observed by the experiment. In addition to the requirement that the IS should be mainly concentrated at negative ω , its SW should be large enough to be observed. As discussed above, this condition is also satisfied by the $t - J$ model.

In summary, we have discussed that dynamical non-double-occupancy effects, which are only obtained be-

yond mean field level, are responsible for a strong asymmetry of the self-energy with respect to $\omega = 0$. This leads to spectral functions where large IS is present at high negative energy with nearly no signals of IS at positive ω . It was also discussed that this picture is very improbable to be obtained from methods which treat the electronic correlations in weak coupling. Our results show similarities with the recent high energy features observed by ARPES experiments in cuprates giving an additional support to the point of view that electronic correlations push cuprates to the strong coupling regime.

Acknowledgments We thank Qiang-Hua Wang for valuable discussions and H. Parent for critical reading the manuscript.

-
- ¹ T. Valla et al., Science **285** 2110 (1999). P.V. Bogdanov et al., Phys. Rev. Lett. **85** 2581 (2000). A. Kaminski et al., Phys. Rev. Lett. **86** 1070 (2001).
- ² Z.-H. Pan *et al.*, arXiv:cond-mat/0610442.
- ³ B. P. Xie *et al.*, Phys. Rev. Lett. **98**, 147001 (2007).
- ⁴ W. Meevasana *et al.*, Phys. Rev. B **75**, 174506 (2007).
- ⁵ J. Graf *et al.*, Phys. Rev. Lett. **98** 067004 (2007).
- ⁶ W. Zhang *et al.*, Phys. Rev. Lett. **101**, 017002 (2008).
- ⁷ See for instance: M. Brunner, F. Assaad, and A. Muramatsu, Phys. Rev B **62** 15480 (2000). E. Dagotto, Rev. Mod. Phys. **66**, 763 (1994).
- ⁸ See for instance: Z. Wang, Int. Journal of Modern Physics B **6**, 155 (1992). P. A. Lee, N. Nagaosa, and X.-G. Wen, Rev. Mod. Phys. **78**, 17 (2006). A. Georges, G. Kotliar, W. Krauth, and J. Rozenberg, Rev. Mod. Phys. **68**, 13 (1996). D. Manske, *The theory of Unconventional Superconductors* (Springer-Verlag, Berlin, 2004).
- ⁹ A. Foussats and A. Greco, Phys. Rev. B **65**, 195107 (2002). A. Foussats and A. Greco, Phys. Rev. B **70**, 205123 (2004).
- ¹⁰ M. Bejas, A. Greco and A. Foussats, Phys. Rev. B **73**, 245104 (2006).
- ¹¹ J. Merino, A. Greco, R. H. McKenzie and M. Calandra, Phys. Rev. B **68**, 245121 (2003).
- ¹² G. Mahan, *Many-Particle Physics* (Plenum Press, New York, 1981).
- ¹³ S. Wakimoto *et al.*, Phys. Rev. Lett. **98**, 277003 (2007). Ph. Bourges, in *The Gap Symmetry and Fluctuations in High Temperature Superconductors*, edited by J. Bok, G. Deutscher, D. Pavuna, S. A. Wolf (Plenum Press, New York, 1998) 349.
- ¹⁴ A. Greco, Phys. Rev. B **77**, 092503 (2008).
- ¹⁵ F. C. Zhang and T. M. Rice, Phys. Rev. B **37**, 3759 (1988)
- ¹⁶ W. Stephan and P. Horsch, Phys. Rev. Lett. **66**, 2258 (1991).
- ¹⁷ A. Moreo, S. Haas, A. W. Sandvik, E. Dagotto, Phys. Rev. B **51** 12045 (1995).
- ¹⁸ Fei Tan and Qiang-Hua Wang, Phys. Rev. Lett. **100**, 117004 (2008).
- ¹⁹ M. M. Zemljič, P. Prelovšek and T. Tohyama, Phys. Rev. Lett. **100**, 036402 (2008).
- ²⁰ D. Manske, I. Eremin, and K.-H. Bennemann, Phys. Rev. Lett. **87**, 177005 (2001). A. Kaminski *et al.*, Phys. Rev. Lett. **86**, 1070 (2001).
- ²¹ A. Lanzara *et al.*, Nature (London) **412**, 510 (2001). R. Zeyher A. Greco, Phys. Rev. B **64**, 140510 (R) (2001). Kulić and O. V. Dolgov, Phys. Rev. B **71**, 092505 (2005).
- ²² H. Castro and G. Deutscher, Phys. Rev. B **73**, 174511 (2004).
- ²³ J. Merino, A. Greco, N. Drichko, and M. Dressell, Phys. Rev. Lett. **96**, 216402 (2006).
- ²⁴ R. S. Markiewicz, S. Sahrakorpi and A. Bansil, Phys. Rev. B **76**, 174514 (2007). A. Macridin, M. Jarrell, T. Maier and D. J. Scalapino, Phys. Rev. Lett. **99**, 237001 (2007).
- ²⁵ A. Greco, Solid State Comm. **142**, 318 (2007).
- ²⁶ D. S. Inosov *et al.*, Phys. Rev. Lett. **99**, 237002 (2007).